Supporting Online Material for

Producing Irreversible Topoisomerase II-Mediated DNA Breaks by Site-Specific Pt(II)-Methionine Coordination Chemistry

Ying-Ren Wang[1], Shin-Fu Chen[1], Chyuan-Chuan Wu[2], Yi-Wen Liao[1], Te-Sheng Lin[1], Ko-Ting Liu[1], Yi-Song Chen[3], Tsai-Kun Li[3,4,*], Tun-Cheng Chien[5,*], and Nei-Li Chan[1,6,*]

[1]Institute of Biochemistry and Molecular Biology, College of Medicine, National Taiwan University, Taipei, Taiwan.

[2]Institute of Molecular Biology, Academia Sinica, Taipei 115, Taiwan.

[3]Department and Graduate Institute of Microbiology, College of Medicine, National Taiwan University, Taipei 100, Taiwan.

[4]Center for Biotechnology, National Taiwan University, Taipei 106, Taiwan.

[5]Department of Chemistry, National Taiwan Normal University, Taipei 116, Taiwan.

[6]Institute of Biochemistry, College of Life Sciences, National Chung Hsing University, Taichung 402, Taiwan.

[*]To whom correspondence should be addressed:

Nei-Li Chan

Institute of Biochemistry and Molecular Biology, College of Medicine, National Taiwan University, Taipei 100, Taiwan. Phone: 886-2-23562214; Fax: 886-2-23915295

Email: nlchan@ntu.edu.tw

Tun-Cheng Chien

Department of Chemistry, College of Science, National Taiwan Normal University, Taipei 116, Taiwan. Phone: 886-2-77346126; Fax: 886-2-29324249

Email: tcchien@ntnu.edu.tw

Tsai-Kun Li

Department and Graduate Institute of Microbiology, College of Medicine, National Taiwan University, Taipei 100, Taiwan. Phone: 886-2-22123456 (ext 88287/88294); Fax: 886-2-23915293

Email: tsaikunli@ntu.edu.tw

This PDF file includes

SUPPLEMENTARY MATERIAL AND METHODS

Construction of recombinant hTop2α^{core}

The coding sequence of hTop2α^{core} (residues 429-1188) was amplified by PCR using the YEpWob6 plasmid (containing the full-length human Top2α gene) (1) as a template and the following oligonucleotide primers:

forward primer: 5'- AGCACGCGTCGACGCTGTAAAACATAATAGAAT -3'

reverse primer: 5'- GCAGTCGAGCTCCATCTTGTTTTTCCTTGGCTT -3'

The restriction sites of *Sal* I and *Sac* I are underlined. The resulting cDNA was cloned into the plasmid pET51b for expression of the recombinant protein with the Strep II tag at the N-terminus and the hexa-His tag at the C-terminus. This plasmid (named 51bDBCCα) was co-transformed with the pLysS plasmid into *Escherichia coli* BL21 (DE3) Star for protein expression.

Expression and purification of recombinant proteins

For expressing human Top2α^{core} and Top2β^{core} (residues 445-1201, (2)), *E. coli* BL21 (DE3) Star-pLysS cells respectively harboring the 51bDBCCα (for Top2α^{core}) or 51bDBCCβ (for Top2β^{core}) plasmid were grown in LB medium at 37 ºC till OD_{600} reached 0.5. Expression of the recombinant protein was induced by adding 0.3 mM isopropyl β-D-1-thiogalactopyranoside (IPTG) to the cell culture. Protein was expressed at 16 ºC for 16 hours. Cells were harvested by centrifugation and then re-suspended in lysis buffer (50 mM sodium phosphate pH 7.4, 10% glycerol, 500 mM NaCl, 5 mM β-mercaptoethanol (β-ME), 0.5 mM phenylmethanesulfonyl fluoride (PMSF), and 10 mM Imidazole). Cells were disrupted by sonication. The crude cell extract was centrifuged at 18,000 rpm for 140 mins at 4 ºC. The resultant supernatant was then applied to a Ni-NTA column. The column was washed to baseline with wash buffer (lysis buffer containing no PMSF), and the bound protein was eluted with elution buffer (wash buffer containing 250 mM Imidazole). The protein was then dialyzed against buffer A (30 mM Tris-HCl pH 7.5, 15 mM NaCl, 2 mM β-ME, and 1 mM EDTA) at 4 ºC for 4 hours, and then loaded onto a HiPrep 16/10 Heparin FF column. The protein was eluted in a linear gradient over 10 column volumes with buffer B (buffer A containing 1 M NaCl). The eluted protein were further purified by a size-exclusion column (Hi-Load Superdex 200). The dimeric hTop2α^{core} or hTop2β^{core} (both with MW about 180 kDa), which represent functional forms of these proteins, were collected and respectively concentrated to 8 or 6.5 mg/ml for the following crystallization procedure. For the size-exclusion purification and protein storage, the gel filtration buffer (50 mM Tris-HCl pH 7.0, 200 mM KCl, 5 mM $MnCl_2$, 1 mM EDTA and 2 mM β-ME) was used for hTop2α^{core}, and the buffer A containing 70 mM NaCl was used for hTop2β^{core}.

For expressing human Top2α$^{\Delta CTD}$ (residues 29-1221) and human Top2β$^{\Delta CTD}$ (residues 45-1201), yeast BCY123 cells respectively harboring the YEpWob6 (for Top2α$^{\Delta CTD}$) (3) and YEphTOP2B (for Top2β$^{\Delta CTD}$) (4) plasmid were streaked on Ura$^-$ plate and grown at 30 ºC for 2 days. Single colonies were picked to grow in 100 ml of SD-U medium (synthetic drop-out medium, lacking

uracil), at 30 ºC for overnight. 10 ml of the overnight culture was then added to 1L SD-U medium and grown at 30 ºC for overnight. Cells were harvested by centrifugation, and resuspended in 100 ml YPG (yeast extract-peptone-glycerol) medium. The 100 ml cells were then added into 10 L YPG medium and grown at 30 ºC for 24 hours. Cells were harvested by centrifugation and resuspended in lysis buffer, and disrupted by bead-beater. The crude cell extract was centrifuged at 20,000 rpm for 180 mins at 4 ºC. The resultant supernatant was applied to a Biorex 70. The column was washed to baseline with wash buffer, and the protein was eluted with elution buffer in a linear gradient over 10 column volumes. The eluted protein was further purified by a size-exclusion column (Hi-Load Superdex 200) in the gel filtration buffer. The dimeric Top2α$^{\Delta CTD}$ or Top2β$^{\Delta CTD}$ (both with MW about 276 kDa) was collected and concentrated to 1.2 μg/μl or 20 ng/μl respectively for the following Top2 cleavage and relaxation assays.

Crystallographic structure refinement of hTop2β^{core}-DNA-etoplatin-N2β and hTop2β^{core}-DNA-etoplatin-N2α complexes

For both structures, initial rigid-body and positional refinement of the MR solutions were performed using phenix.refine with default settings (5). The resulting F_o-F_c maps showed clearly the presence of bound etoplatins and allowed the three main components of etoplatins (the aglycone core, E-ring and dichlorodiammineplatinum(II) moiety; see Figure 1) to be placed manually in Coot (6) (Figure 3). For the etoplatin-N2β-bound structure (hTop2β^{core}-DNA-etoplatin-N2β), the F_o-F_c density corresponding to the dichlorodiammineplatinum(II) moiety extends towards and connects to the side-chain thioether group of M782. Because the spatial position of the M782 side-chain S$^{\delta}$ overlaps closely with one of the Pt^{2+}-coordinating Cl^- ions, we reasoned that this S$^{\delta}$ has replaced a Cl^- and become liganded to Pt^{2+}, forming a Met-Pt^{2+} complex that chemically resembles the [*cis*-Pt(NH_3)$_2$(S)(Cl)]$^-$ compounds observed previously (7). Although the bond lengths and coordination geometry of the Pt^{2+} center cannot be unambiguously specified at the current resolution (2.57 Å, Table 1), the electron-rich Pt^{2+} ions can nevertheless be positioned precisely in the F_o-F_c maps given the extremely intense positive peaks (Supplementary Figure S8A and B). A reasonably exhaustive survey of four-coordinated Pt(II) complexes with a PtA_2BC coordination pattern (7), in which A, B and C correspond to nitrogen, sulfur and chloride, respectively, revealed that the four ligands should adopt a slightly distorted square planar arrangement with respect to the spatially well-defined Pt^{2+}. Therefore, the positions of Pt^{2+}-coordinating atoms were manually adjusted in Coot such that the bond lengths and bond angles approximate the averaged values observed in PtA_2BC complexes. Specifically, the Pt^{2+}-N, Pt^{2+}-S and Pt^{2+}-Cl^- bond lengths were restrained to 2.0, 2.3 and 2.3 Å, respectively, and the four ligands were restrained to adopt a square planar arrangement about the central Pt^{2+} during subsequent refinement cycles. Unlike the heavier S and Cl^- ligands, the two Pt^{2+}-coordinating nitrogen atoms lack well defined electron densities in the F_o-F_c maps (Supplementary Figure S8C), likely because signals from these light atoms are masked by the electron-rich Pt^{2+}, nevertheless, the refined structure of etoplatin-N2β fits the corresponding difference density reasonably well (Supplementary Figure S8D). The structure of hTop2β^{core}-DNA-etoplatin-N2α was refined using a similar

procedure by restraining dichlorodiammineplatinum(II) moiety in a square planar geometry and the Pt^{2+}-N and Pt^{2+}-Cl^{-} bond lengths to 2.0 and 2.3 Å, respectively. Detailed data collection and refinement parameters are summarized in Table 1.

Also note that we did not specify the chirality of the diammine linker during the synthesis of etoplatin-N2β and N2α. Therefore, for each anomer, it is likely that one of the two possible stereoisomers may bind tighter to the crystallized Top2cc. To examine whether a particular stereoisomer was enriched in the Top2cc crystals, the two stereoisomers associated with the N2β (or N2α) anomer were modeled either individually or simultaneously in 0.5 occupancy to the electron density maps, followed by additional refinement cycles with phenix.refine. We concluded that both stereoisomers can be modeled equally well at the present resolution (Supplementary Figure S9).

SUPPLEMENTARY FIGURES

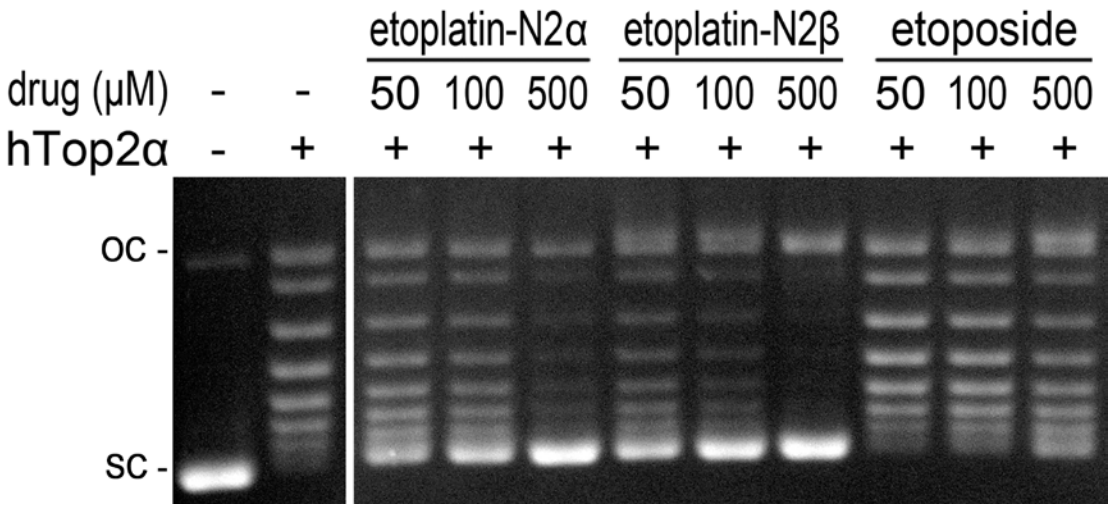

Figure S1. Inhibition of the relaxation activity of hTop2α by etoposide and etoplatins. Each relaxation reaction contains 300 ng of supercoiled (SC) pRYG plasmid DNA. The enzyme-positive reactions contain 120 ng of hTop2α$^{\Delta CTD}$, a fully active proxy for hTop2α. OC stands for open circle (fully-relaxed product produced by Top2) DNA. Similar to the result shown in Figure 2A, etoplatin-N2β, but not the N2α epimer, more potently inhibits the relaxation activity of hTop2α compared to etoposide.

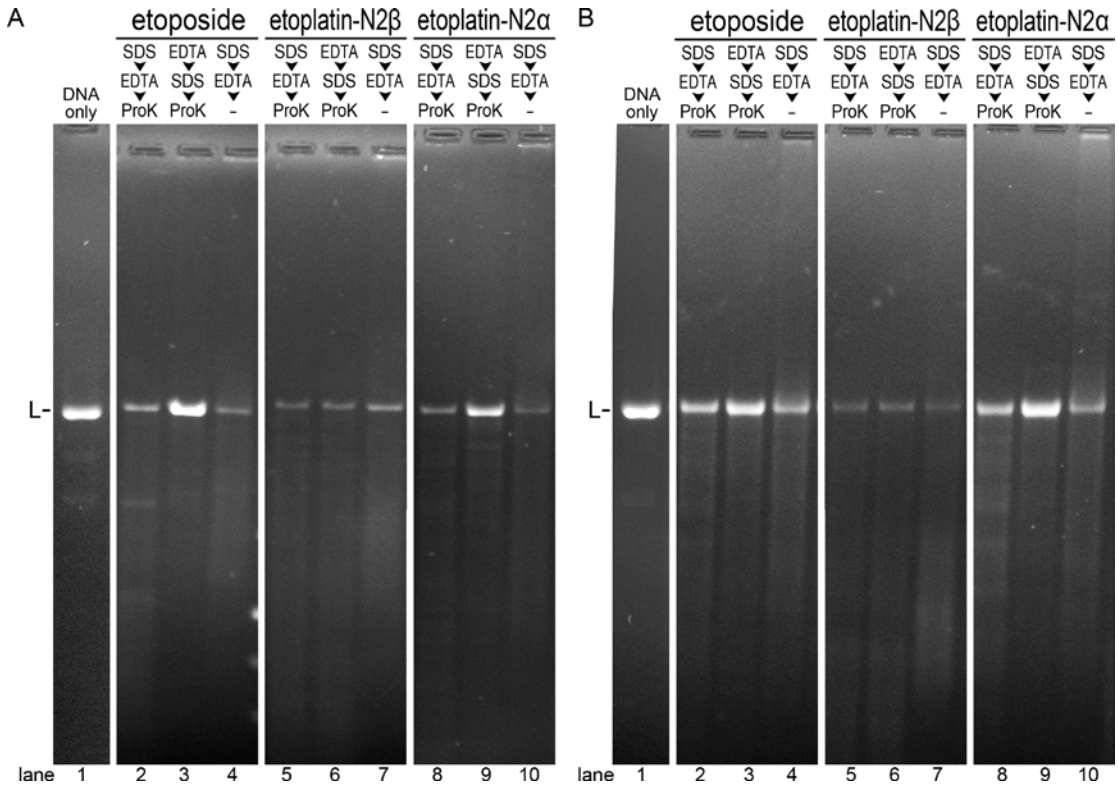

Figure S2. DNA cleavage assay showing the formation of EDTA-resistant DNA breaks mediated by hTop2β (A) and 2α (B) in the presence of etoplatin-N2β. This is the full-sized image of the cropped agarose gel shown in Figure 2B to show the cleaved DNA smear (below the linear DNA substrate) and the Top2-linked DNA (DNA retained in the wells and smear above the linear DNA substrate) in the reactions without proteinase K treatment. The disappearance and reemergence of the linear substrate DNA (L) indicate the production and resealing of DNA breaks, respectively. The fully active hTop2β$^{\Delta CTD}$ and hTop2α$^{\Delta CTD}$ were used as proxies for hTop2β and hTop2α, respectively, in this assay.

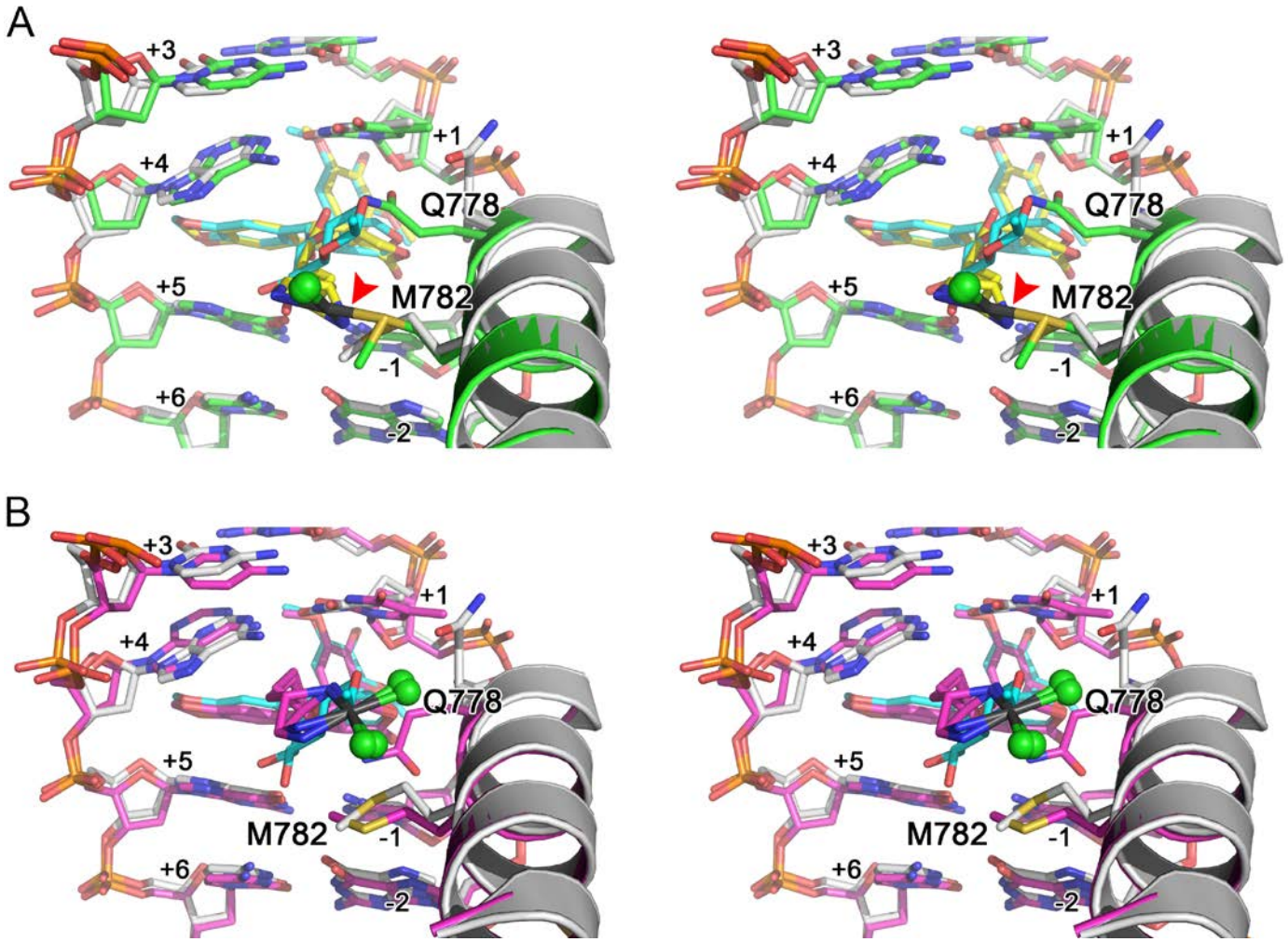

Figure S3. Structural superimposition of the hTop2β^{core}-derived cleavage complex stabilized by etoposide (PDBid: 3QX3, (2)) and the ones stabilized by etoplatin-N2β (A) and -N2α (B). In both panels, the parental etoposide-bound structure is shown in gray, and the newly determined structures bound by etoplatin-N2β and -N2α are colored in green and purple, respectively. The bound etoposide in the parental structure is shown in cyan stick representation, and etoplatin-N2β and -N2α are in yellow stick representation. Regardless of the bound drug, the protein parts of these structures are resonably well aligned, indicating the lack of significant structural changes upon drug replacement. It is noteworthy that the Q778 and M782 side chains adopt different rotamer conformations in response to the presence of a stereochemically distinct Pt^{2+}-coordinating diammine linker of etoplatin-N2α and N2β.

A

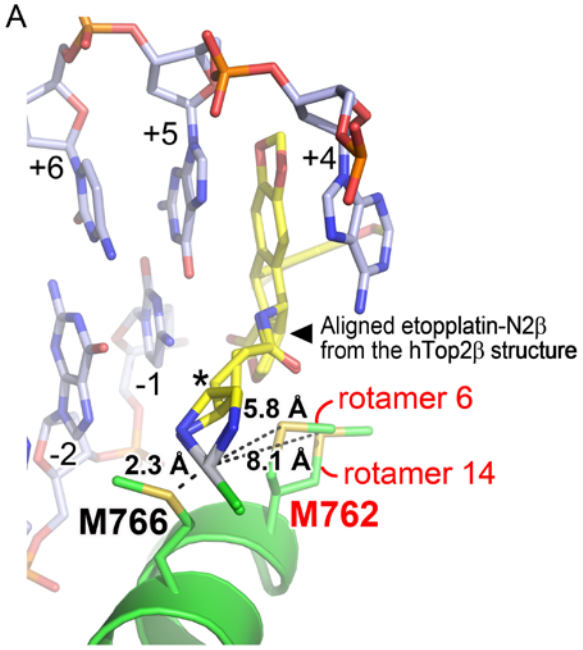

M762 Rotamer #	Chi 1	Chi 2	Chi 3	Pt – Met(S$^{\delta}$) (Å)
1	-36.8	-50.8	161.8	8.8
2	-68.7	-68.7	-68.7	7.3
3	-61.2	176.3	176.3	8.1
4	-72.5	-72.5	74.7	7.1
5	180.0	-70.0	60.7	4.5
6	176.3	176.3	-62.0	5.8
7	-72.5	74.7	106.9	9.4
8	-70.0	60.7	180.0	9.4
9	-68.7	-68.7	-171.9	7.3
10	176.3	-62.0	172.5	4.5
11	74.7	106.9	-72.5	5.8
12	60.7	180.0	-70.0	7.5
13	-68.7	-171.9	-171.9	7.7
14	-62.0	172.5	172.5	8.1

B

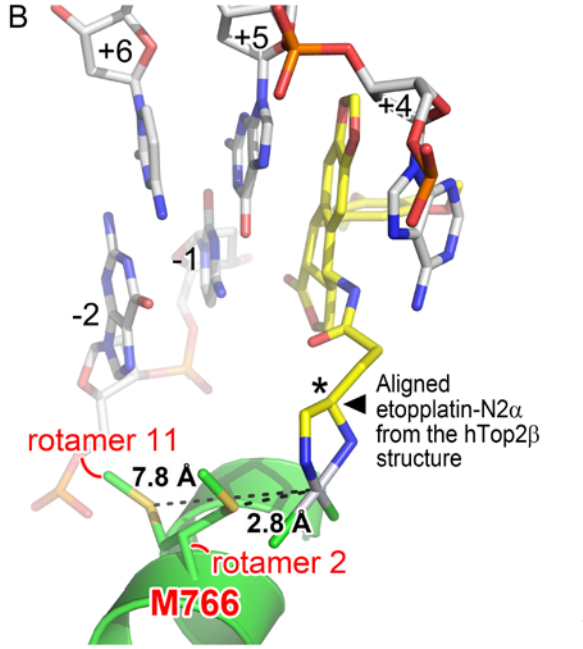

M766 Rotamer #	Chi 1	Chi 2	Chi 3	Pt – Met(S$^{\delta}$) (Å)
1	-90.2	-104.3	-37.0	4.0
2	-68.7	-68.7	-68.7	2.8
3	-61.2	176.3	176.3	4.4
4	-72.5	-72.5	74.7	3.0
5	180.0	-70.0	60.7	7.2
6	176.3	176.3	-62.0	6.2
7	-72.5	74.7	106.9	3.9
8	-70.0	60.7	180.0	3.8
9	-68.7	-68.7	-171.9	2.8
10	176.3	-62.0	172.5	7.2
11	74.7	106.9	-72.5	7.8
12	60.7	180.0	-70.0	7.2
13	-68.7	-171.9	-171.9	4.2
14	-62.0	172.5	172.5	4.4

C

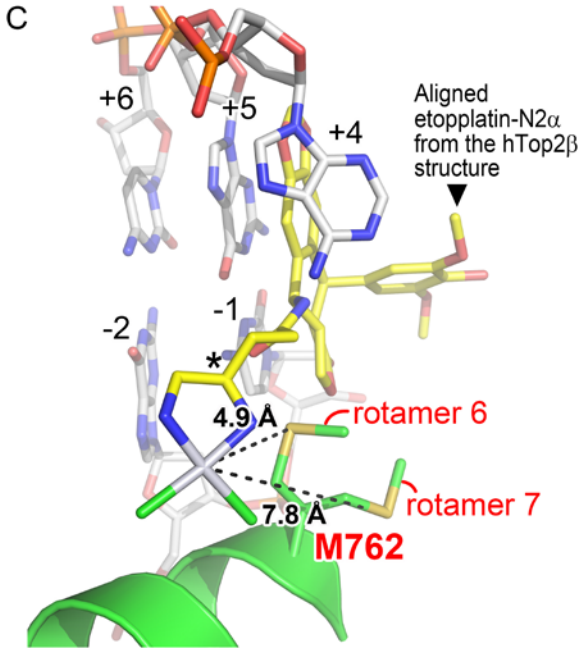

M762 Rotamer #	Chi 1	Chi 2	Chi 3	Pt – Met(S$^{\delta}$) (Å)
1	-61.9	-172.5	172.49	6.8
2	-68.7	-68.7	-68.7	5.3
3	-61.2	176.3	176.3	6.7
4	-72.5	-72.5	74.7	5.0
5	180.0	-70.0	60.7	4.3
6	176.3	176.3	-62.0	4.9
7	-72.5	74.7	106.9	7.8
8	-70.0	60.7	180.0	7.8
9	-68.7	-68.7	-171.9	5.3
10	176.3	-62.0	172.5	4.3
11	74.7	106.9	-72.5	5.7
12	60.7	180.0	-70.0	7.0
13	-68.7	-171.9	-171.9	6.3
14	-62.0	172.5	172.5	6.8

Figure S4. Structural models of the hTop2α cleavage complexes stabilized by etoplatins. (A) The modeled structure of hTop2α^{core}-DNA-etoplatin-N2β revealed that the side-chain S$^{\delta}$ of M766 (equivalent to M782 of hTop2β) may contact the coordination sphere of Pt^{2+} to allow the formation of a Pt^{2+}-S coordinate bond (left), consistent with the finding that etoplatin-N2β acts as an irreversible poison of hTop2α. In contrast, Pt^{2+} is not likely to form a coordinate bond with M762 because, for all possible rotamers, the positions of its side-chain S$^{\delta}$ are too distant to react with Pt^{2+} (right). (B, C) The modeled structure of hTop2α^{core}- DNA-etoplatin-N2α suggests that neither M766 nor M762 would form coordinate bond with the Pt^{2+} of etoplatin-N2α. For all possible rotamers, the estimated distances between Pt^{2+} and the S$^{\delta}$ of M766 (B, right) and M762 (C, right) are too long to allow coordinate bond formation. For simplicity, only selected rotamers whose S$^{\delta}$ points directly at Pt^{2+} without the presence of intervening ε methyl group are shown.

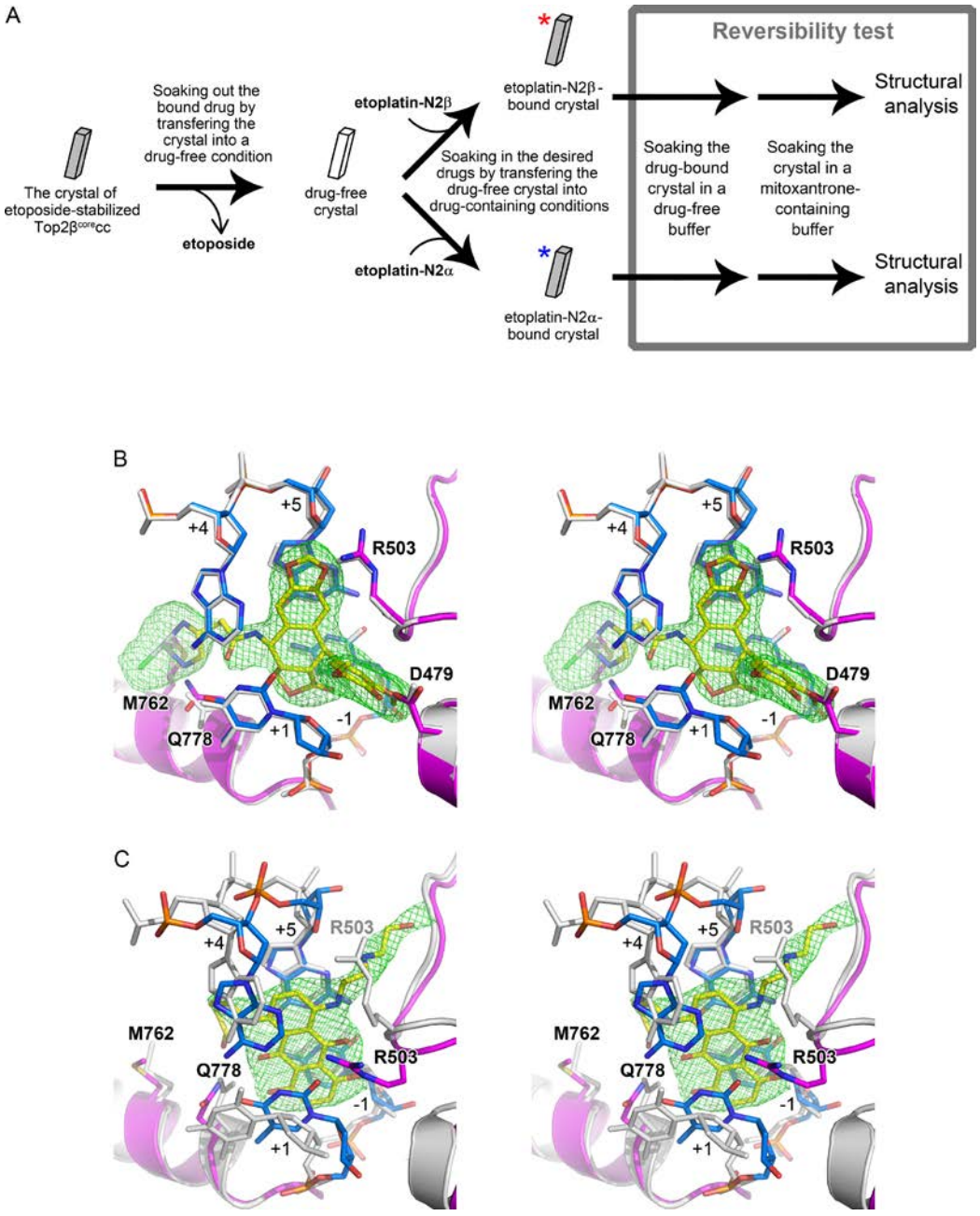

Figure S5. Examining the susceptibility of the bound etoplatin-N2β and N2α to drug replacement. (A) The experimental scheme for drug replacement and reversibility test. (B and C) The resultant omit (mF_o-DF_c) electron density maps of the bound drug (at 3.0 σ, in green meshes) after subjecting the etoplatin-N2β (or N2α) bound hTop2β^{core}-DNA crystals (marked with red and blue asterisks, respectively, in panel A) to the reversibility test. The resulting electron density maps show clearly that etoplatin-N2β is resistant to drug replacement and remained tightly bound (B), while etoplatin-N2α dissociated from the drug binding site and was replaced by mitoxantrone (C). The parental etoplatin-N2α and -N2β-bound structures and the post-soaking structures are shown in gray and purple, respectively. DNA of the resultant structures are shown in blue sticks representation. The bound etoplatin-N2β (resolution 2.5 Å, panel B) and mitoxantrone (resolution 2.4 Å, panel C) were modeled according to the features shown in the omit maps and are displayed in yellow sticks representation. The observed repositioning of the R503 side chain upon the binding of mitoxantrone was also detected in the mitoxantrone-bound hTop2βcc structure determined previously (8).

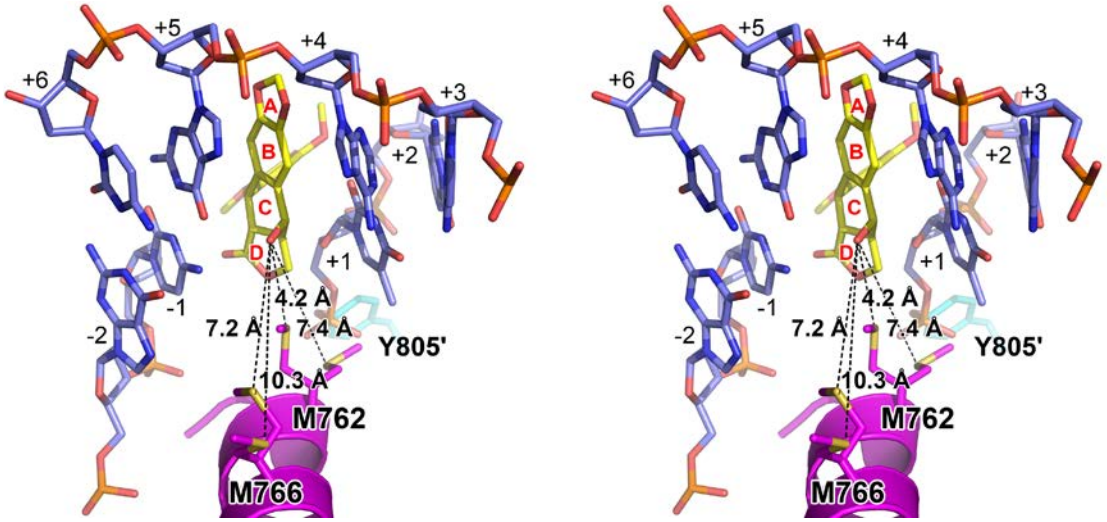

Figure S6. Stereo view of the major groove-binding pocket in the structure of hTop2α^{core}-derived cleavage complex stabilized by etoposide. DNA is shown in blue sticks representation. Protein is shown in cartoon/stick presentation with the two polypeptide chains colored differently (magenta and cyan). For clarity of viewing, the sugar moiety of the bound etoposide (yellow sticks representation) is omitted from the model. Depending on rotamer conformations adopted by the methionine side chains, the estimated distances between the C-ring-attached hydroxyl group of the bound etoposide and the sulfur atoms of the flanking methionines (M762: 4.2-7.4 Å; M766: 7.2-10.3 Å) are labeled and illustrated by the black dashed lines. Given that M762 and M766 occupy distinct spatial locations, it may be feasible to design a site-specific methionine-targeting by adjusting the length of the Pt^{2+}-coordinating diammine linker such that Pt^{2+} specifically coordinates with M762, which would allow for hTop2α-selective targeting.

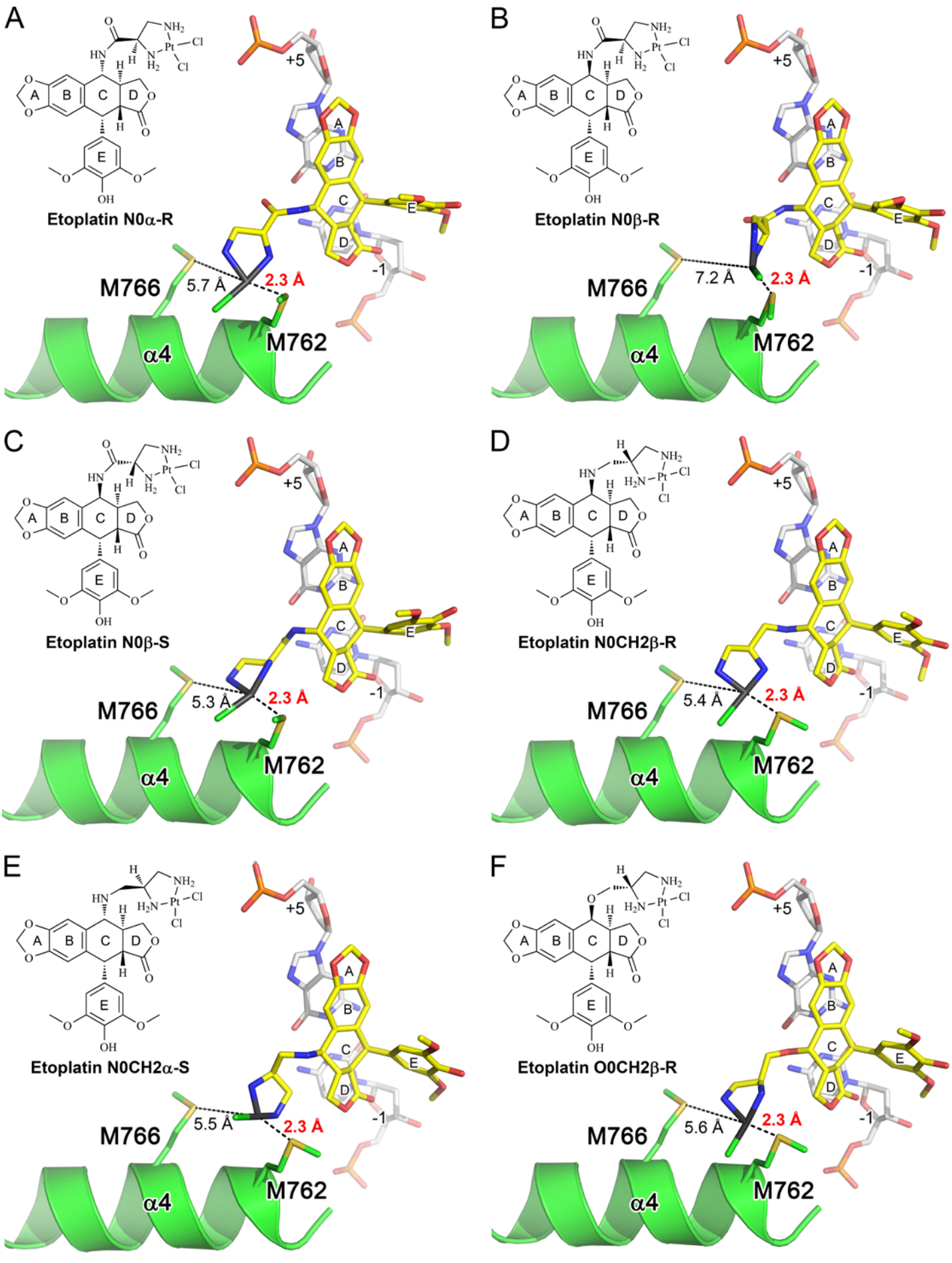
A
Etoplatin N0α-R
+5
A
B
C
D
E
-1
M766
5.7 Å
2.3 Å
M762
α4
B
Etoplatin N0β-R
+5
M766
7.2 Å
2.3 Å
M762
α4
C
Etoplatin N0β-S
+5
M766
5.3 Å
2.3 Å
M762
α4
D
Etoplatin N0CH2β-R
+5
M766
5.4 Å
2.3 Å
M762
α4
E
Etoplatin N0CH2α-S
+5
M766
5.5 Å
2.3 Å
M762
α4
F
Etoplatin O0CH2β-R
+5
M766
5.6 Å
2.3 Å
M762
α4

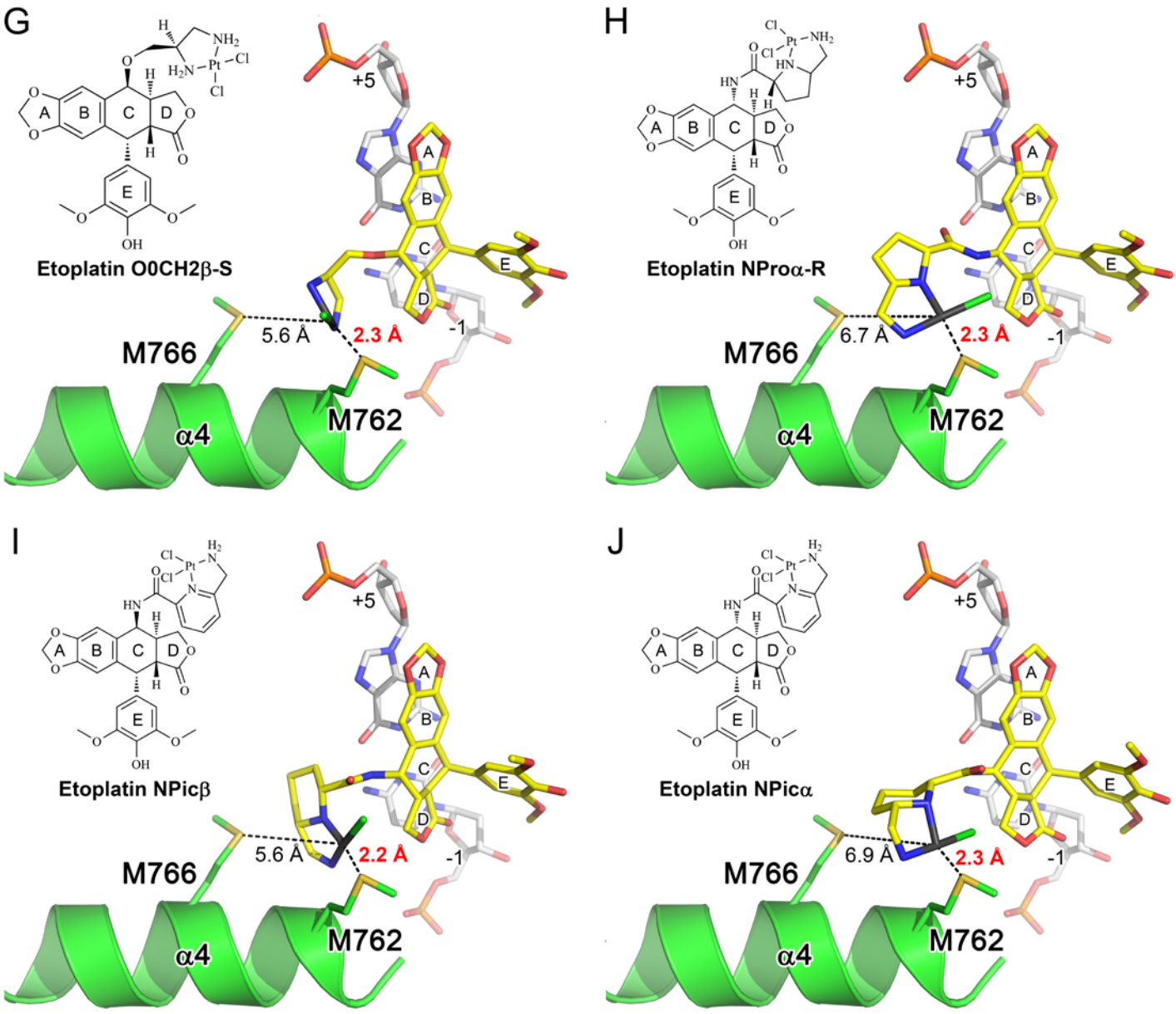

Figure S7. Simulated targeting of the hTop2α-specific M762 by newly designed etoplatins. (A~J) Each panel shows the structure and a simulated binding mode of a synthesizable, new generation of etoplatin. The etoplatins are colored by atom type (carbon, yellow; oxygen, red; nitrogen, blue; sulfur, yellow; chloride, green; Pt^{2+}, dark grey).This modeling analysis showed that, by adjusting the linker structure and length, Pt^{2+} can be delivered to ~2.3 Å from the S^{δ} of M762 to allow coordinate bond formation. In contrast, the S^{δ} of M766 was found to lie at least 5 Å away from Pt^{2+} and thus unable to serve as a ligand.

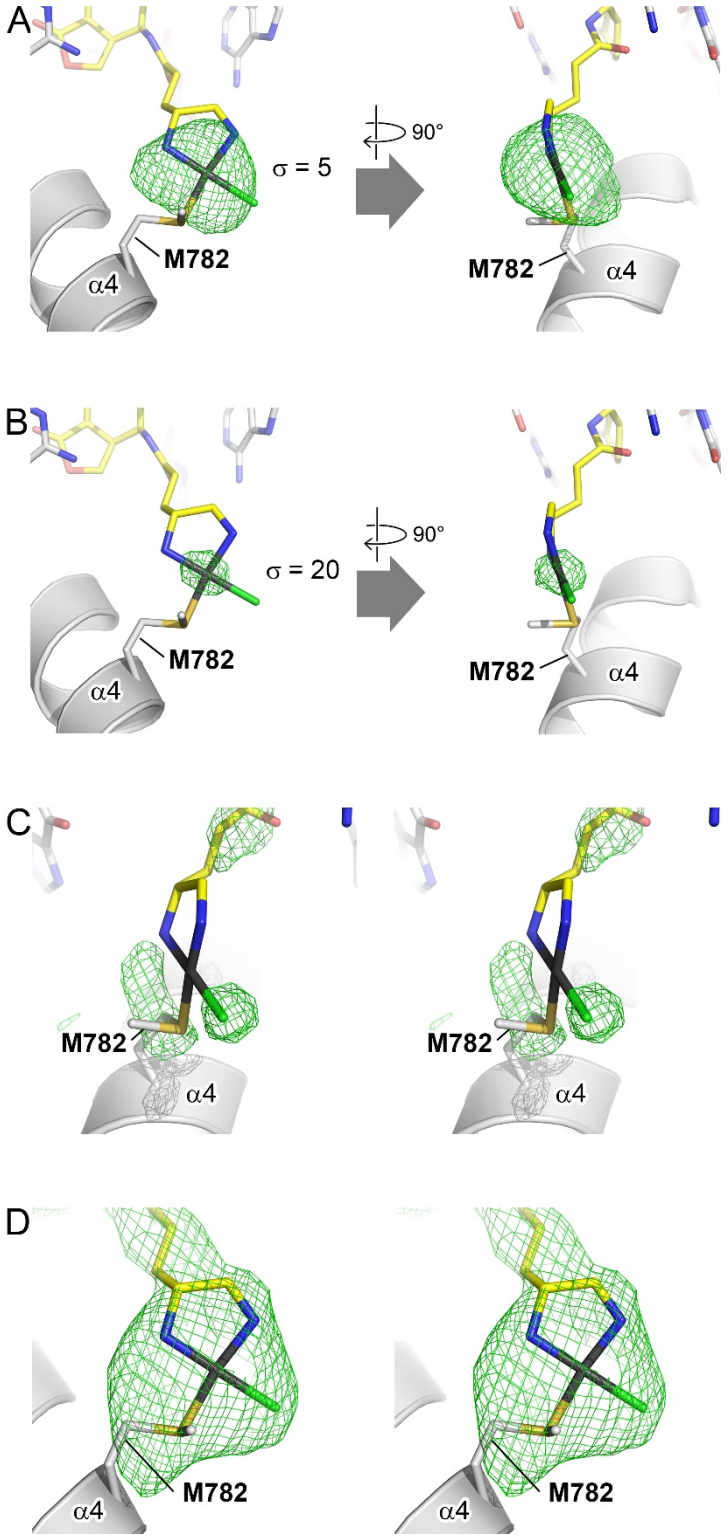

Figure S8. Unbiased F_o-F_c maps illustrating the Pt(II) coordination geometry observed in hTop2β^{core}-DNA-etoplatin-N2β. (A, B) The F_o-F_c map calculated by deleting the Pt^{2+} coordinates in the model at 5 (A) and 20 (B) σ shows clearly the positions of Pt^{2+} ions in the structure. (C) Stereo view of the F_o-F_c map (contoured at 5 σ) calculated by mutating M782 to alanine and by retaining just the Pt^{2+} while deleting all non-metal atoms of etoplatin-N2β shows the positions of the M782 side-chain, Cl^-, and portion of the diammine linker in the structure. (D) Stereo view of the F_o-F_c map (contoured at 3 σ) calculated by mutating M782 to alanine and by deleting the entire etoplatin-N2β shows the four-coordinated Pt(II) center can be described reasonably well by a square planar geometry.

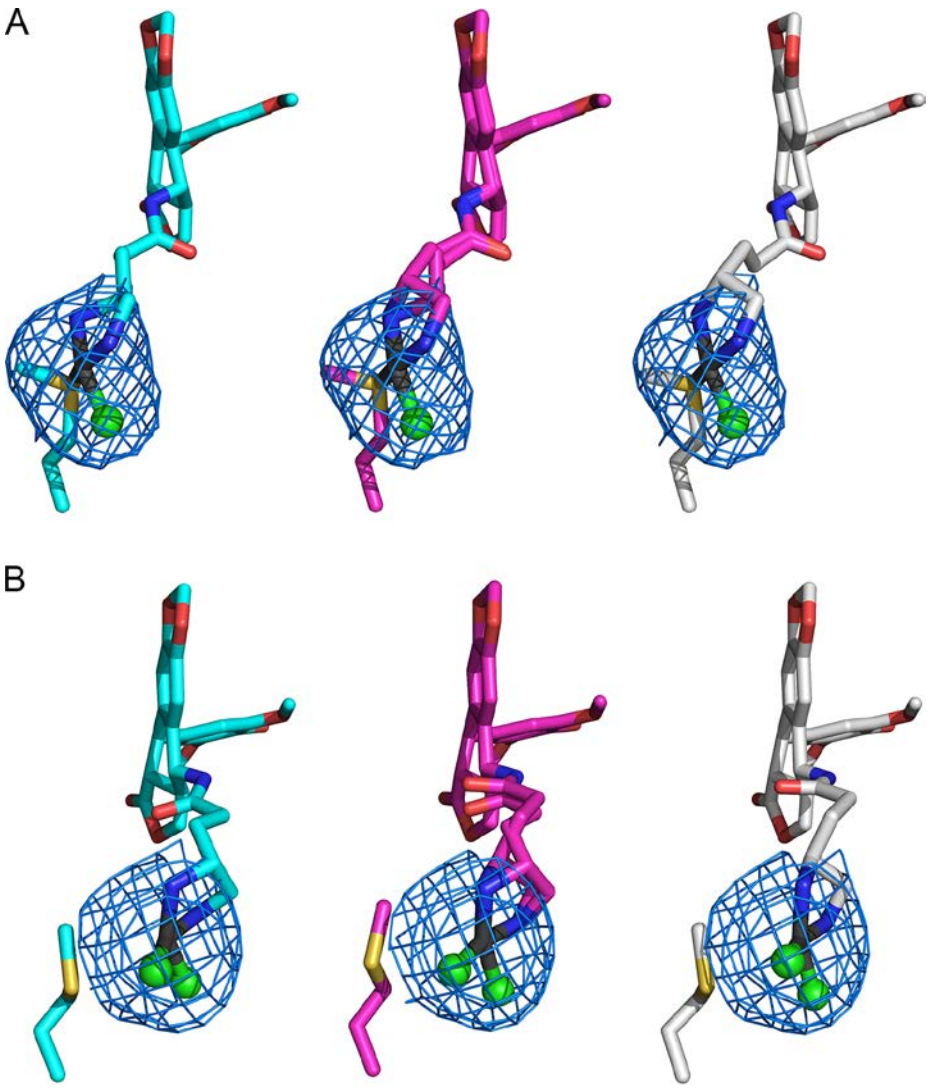

Figure S9. The electron density maps observed for the cis-dichlorodiammineplatinum(II) moiety of etoplatin-N2β and N2α can be fitted equally well by both diastereomers associated with each etoplatin. Because the chirality of the diammine linker was not specified during the synthesis of etoplatin-N2β and N2α. Therefore, it is possible that a particular stereoisomer may be enriched in the crystals of hTop2β^{core}-derived cleavage complex, two possible stereoisomers of etoplatin-N2β (A) and -N2α (B) were individually modeled (left and right panels) or simultaneously in 0.5 occupancy (middle panel) to the F_o-F_c electron density map, followed by additional refinement cycles. We concluded that both stereoisomers can be modeled equally well at the present resolution.

SUPPLEMENTARY TABLES

Table S1. Etoplatin-N2β exhibits a better cancer cell-killing activity than that of Etoplatin-N2α in a hTop2-dependent manner

Drugs	Cytotoxicity (IC_{50}, μM)	
	HL-60	HL-60/MX2
Etoposide	0.107 ± 0.01*	4.65 ± 2.4
Etoplatin-N2β	27.49 ± 5.0	>100
Etoplatin-N2α	>100	>100

* Mean ± SD

SUPPLEMENTARY SCHEMES

Scheme S1. Synthesis of platinum(II)-4,5-diaminovaleric acid complex ($PtCl_2$(*N*,*N*-Dav)) (2)

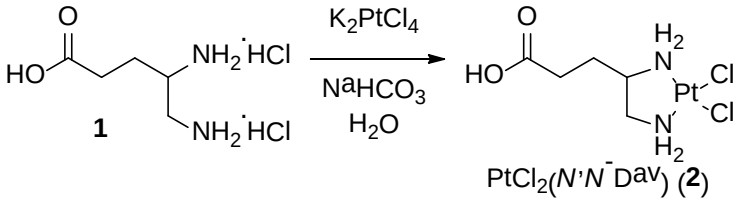

Platinum(II)-4,5-diaminovaleric acid complex ($PtCl_2$(*N*,*N*-Dav)) (2) (9)

To a mixture of 4,5-diaminovaleric acid dihydrochloride (**1**, 250 mg, 1.22 mmol) in H_2O (10 mL) was added $NaHCO_3$ (205 mg, 2.44 mmol). The mixture was stirred at room temperature for 10 min then K_2PtCl_4 (0.506 g, 1.22 mmol, 1 equiv) was added. The reaction mixture was heated at 80 ^oC under N_2 overnight. The reaction mixture was cooled to room temperature and a yellow solid formed. The precipitate was filtered and dried to give a yellow solid (320 mg). The crude product was used for the subsequent reaction without further purification.

Scheme S2. Synthesis of etoplatin-N2β (5β)

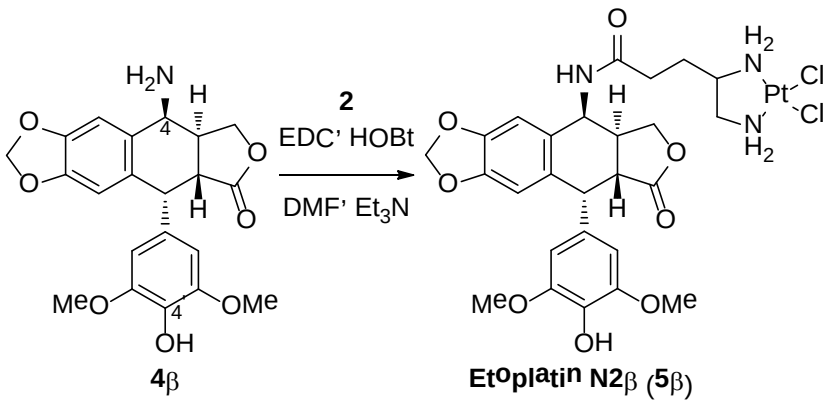

Etoplatin-N2β (5β)

To a mixture of $PtCl_2$(*N*,*N*-Dav) (9) (**2**, 239 mg, 0.6 mmol), (*4S*)-4-amino-4-deoxy-4'-*O*-demethylpodophyllotoxin (10) (**4β**, 200 mg, 0.5 mmol), EDC (144 mg, 0.75 mmol) and HOBt (108 mg, 0.8 mmol) in DMF (15 mL) was added Et_3N (101 mg, 1.0 mmol) at room temperature. The mixture was stirred at room temperature overnight. The reaction mixture was extracted with ethyl acetate and the organic layer was concentrated. The crude product was purified by preparative HPLC (acetonitrile/H_2O, 15-40%, 25 min) to give **Etoplatin N2β** (**5β**, yellow solid, 160 mg, 41%). ^{1}H NMR (DMSO-d_6, 400 MHz, ppm) δ 8.25 (s, 1 H), 8.22 (d, 1 H, *J* = 8.2 Hz), 6.77 (s, 1 H), 6.53 (s, 1 H), 6.24 (s, 2 H), 6.02 (s, 1 H), 5.99 (s, 1 H), 5.54-5.53 (m, 1 H), 5.36-5.29 (m, 2 H), 5.15 (dd, 1 H, *J* = 4.6, 8.1 Hz), 5.08 (t, 1 H, *J* = 9.7 Hz), 4.49 (d, 1 H, *J* = 5.1 Hz), 4.27 (t, 1 H, *J* = 8.0 Hz), 3.70 (dd, 1 H, *J* = 8.9, 10.6 Hz), 3.63 (s, 6 H), 3.12 (dd, 1 H, *J* = 5.2, 14.4 Hz), 2.97-2.89 (m, 1 H), 2.60-2.57 (m, 1 H), 2.37-2.35 (m, 1 H), 2.20-2.12 (m, 3 H), 1.81-1.74 (m, 2 H); ^{13}C NMR (DMSO-d_6, 100 MHz, ppm) δ 174.87, 171.89, 147.61, 146.98, 135.23, 132.62, 130.83, 130.56, 109.84, 109.40, 109.00, 101.65, 68.77, 59.67, 56.47, 50.88, 47.09, 43.30, 41.37, 36.95, 32.48, 26.95; MS (ESI) m/z 780 (100) (M+2); HRMS (ESI, TOF) calcd for $C_{26}H_{31}Cl_2N_3O_8Pt$ (M^+): 778.1136. Found: 778.1124.

Scheme S3. Synthesis of etoplatin-N2α (5α)

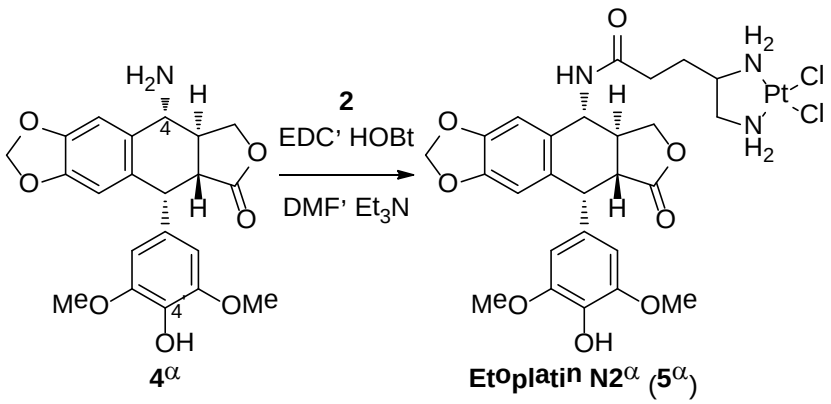

Etoplatin-N2α (5α)

To a mixture of $PtCl_2$(*N*,*N*-Dav) (9) (**2**, 239 mg, 0.6 mmol), (*4R*)-4-amino-4-deoxy-4'-*O*-demethylpodophyllotoxin (10) (**4α**, 200 mg, 0.5 mmol), EDC (144 mg, 0.75 mmol) and HOBt (108 mg, 0.8 mmol) in DMF (15 mL) was added Et_3N (101 mg, 1.0 mmol) at room temperature. The mixture was stirred at room temperature overnight. The reaction mixture was extracted with ethyl acetate and the organic layer was concentrated. The crude product was purified by preparative HPLC (acetonitrile/H_2O, 15-40%, 25 min) to give **Etoplatin N2α** (**5α**, pale yellow solid, 150 mg, 38%). ^{1}H NMR (DMSO-d_6, 400 MHz, ppm) δ 8.45 (d, 1 H, *J* = 8.0 Hz), 8.25 (s, 1 H), 6.81 (s, 1 H), 6.52 (s, 1 H), 6.36 (s, 2 H), 5.99 (s, 2 H), 5.53-5.51 (m, 1 H), 5.35-5.31 (m, 2 H), 5.11 (t, 1 H, *J* = 9.4 Hz), 4.95 (t, 1 H, *J* = 9.1 Hz), 4.47 (d, 1 H, *J* = 4.6 Hz), 4.30 (t, 1 H, *J* = 7.6 Hz), 4.06 (t, 1 H, *J* = 9.6 Hz), 3.68 (s, 6 H), 3.23 (dd, 1 H, *J* = 4.9, 14.2 Hz), 2.69-2.61 (m, 2 H), 2.37-2.31 (m, 1 H), 2.29-2.24 (m, 2 H), 2.16-2.15 (m, 1 H), 1.89-1.75 (m, 2 H); ^{13}C NMR (DMSO-d_6, 100 MHz, ppm) δ 175.00, 172.69, 147.60, 146.96, 135.29, 132.46, 131.58, 131.33, 110.19, 109.47, 106.71, 101.57, 71.09, 59.59, 56.78, 51.66, 51.18, 45.26, 43.50, 38.85, 32.60, 27.00; MS (ESI) m/z 780 (100) (M+2); HRMS (ESI, TOF) calcd for $C_{26}H_{31}Cl_2N_3O_8Pt$ (M^+): 778.1136. Found: 778.1133.

SUPPLEMENTARY REFERENCES

1. Wasserman, R.A., Austin, C.A., Fisher, L.M. and Wang, J.C. (1993) Use of yeast in the study of anticancer drugs targeting DNA topoisomerases: expression of a functional recombinant human DNA topoisomerase II alpha in yeast. *Cancer Res.*, **53**, 3591-3596.
2. Wu, C.C., Li, T.K., Farh, L., Lin, L.Y., Lin, T.S., Yu, Y.J., Yen, T.J., Chiang, C.W. and Chan, N.L. (2011) Structural basis of type II topoisomerase inhibition by the anticancer drug etoposide. *Science*, **333**, 459-462.
3. Austin, C.A., Marsh, K.L., Wasserman, R.A., Willmore, E., Sayer, P.J., Wang, J.C. and Fisher, L.M. (1995) Expression, domain structure, and enzymatic properties of an active recombinant human DNA topoisomerase II beta. *J. Biol. Chem.*, **270**, 15739-15746.
4. Chen, Y.T., Collins, T.R., Guan, Z., Chen, V.B. and Hsieh, T.S. (2012) Probing conformational changes in human DNA topoisomerase IIalpha by pulsed alkylation mass spectrometry. *J. Biol. Chem.*, **287**, 25660-25668.
5. Adams, P.D., Afonine, P.V., Bunkoczi, G., Chen, V.B., Davis, I.W., Echols, N., Headd, J.J., Hung, L.W., Kapral, G.J., Grosse-Kunstleve, R.W. *et al.* (2010) PHENIX: a comprehensive Python-based system for macromolecular structure solution. *Acta Crystallogr. D, Biol. Crystallogr.*, **66**, 213-221.
6. Emsley, P., Lohkamp, B., Scott, W.G. and Cowtan, K. (2010) Features and development of Coot. *Acta Crystallogr. D, Biol. Crystallogr.*, **66**, 486-501.
7. Melnik, M. and Mikus, P. (2014) Structure aspects of monomeric platinum coordination complexes. *Mater. Sci. Appl.*, **5**, 512-547.
8. Wu, C.C., Li, Y.C., Wang, Y.R., Li, T.K. and Chan, N.L. (2013) On the structural basis and design guidelines for type II topoisomerase-targeting anticancer drugs. *Nucleic Acids Res.*, **41**, 10630-10640.
9. Altman, J., Wilchek, M. and Warshawsky, A. (1985) Platinum(II) complexes with 2,4-diaminobutyric acid, ornithine, lysine and 4,5-diaminovaleric acid. *Inorg. Chim. Acta.*, **107**, 165-168.
10. Hansen, H.F., Jensen, R.B., Willumsen, A.M., Norskovlauritsen, N., Ebbesen, P., Nielsen, P.E. and Buchardt, O. (1993) New compounds related to podophyllotoxin and congeners: synthesis, structure elucidation and biological testing. *Acta. Chem. Scand.*, **47**, 1190-1200.